
# NAVAL POSTGRADUATE SCHOOL

**MONTEREY, CALIFORNIA**

# THESIS

**LONG-RANGE FORECASTING OF THE ONSET OF SOUTHWEST MONSOON WINDS AND WAVES NEAR THE HORN OF AFRICA**

by

Gary M. Vines

December 2017

Thesis Advisor: Tom Murphree
Co-Advisor: Megan Hutchins

THIS PAGE INTENTIONALLY LEFT BLANK

| REPORT DOCUMENTATION PAGE | | | *Form Approved OMB No. 0704-0188* |
|---|---|---|---|
| Public reporting burden for this collection of information is estimated to average 1 hour per response, including the time for reviewing instruction, searching existing data sources, gathering and maintaining the data needed, and completing and reviewing the collection of information. Send comments regarding this burden estimate or any other aspect of this collection of information, including suggestions for reducing this burden, to Washington headquarters Services, Directorate for Information Operations and Reports, 1215 Jefferson Davis Highway, Suite 1204, Arlington, VA 22202-4302, and to the Office of Management and Budget, Paperwork Reduction Project (0704-0188) Washington, DC 20503. | | | |
| **1. AGENCY USE ONLY** ***(Leave blank)*** | **2. REPORT DATE** December 2017 | **3. REPORT TYPE AND DATES COVERED** Master's thesis | |
| **4. TITLE AND SUBTITLE** **LONG-RANGE FORECASTING OF THE ONSET OF SOUTHWEST MONSOON WINDS AND WAVES NEAR THE HORN OF AFRICA** | | | **5. FUNDING NUMBERS** |
| **6. AUTHOR(S)** Gary M. Vines | | | |
| **7. PERFORMING ORGANIZATION NAME(S) AND ADDRESS(ES)** Naval Postgraduate School Monterey, CA 93943-5000 | | | **8. PERFORMING ORGANIZATION REPORT NUMBER** |
| **9. SPONSORING /MONITORING AGENCY NAME(S) AND ADDRESS(ES)** N/A | | | **10. SPONSORING / MONITORING AGENCY REPORT NUMBER** |
| **11. SUPPLEMENTARY NOTES** The views expressed in this thesis are those of the author and do not reflect the official policy or position of the Department of Defense or the U.S. Government. IRB number ____N/A____. | | | |
| **12a. DISTRIBUTION / AVAILABILITY STATEMENT** Approved for public release. Distribution is unlimited. | | | **12b. DISTRIBUTION CODE** |

**13. ABSTRACT (maximum 200 words)**

The Asian southwest monsoon (SWM) east of the Horn of Africa (HOA) is important in planning and conducting maritime operations in this region. Skillful subseasonal to seasonal (S2S) forecasts of the SWM onset are needed for operational planning but are not yet available. We investigated the potential for S2S forecasting of the onset of SWM surface winds and ocean surface waves off HOA by analyzing global atmospheric and oceanic variables, and three onset states: early, normal, and late. We identified relationships between variables, precursor conditions for each state, and potential predictors for each state. We used the predictors to conduct 48 years of hindcasting. We assessed the skill of the hindcasts and identified two Pacific sea surface temperature (SST) predictors with a high potential to contribute to S2S forecasts of the onset. These results indicate that El Niño / La Niña (ENLN) variations are important in generating early, normal, and late onsets, but are not the only factors. The mechanisms that link remote SSTs to the onset appear to involve anomalous tropical Rossby-Kelvin waves that extend across the western tropical Pacific and the Indian Ocean–south Asian regions.

| **14. SUBJECT TERMS** climate, climate variations, climate analysis, long-range forecasting, subseasonal to seasonal, Horn of Africa, Somali Jet, Indian Ocean, maritime continent, south Asia, southwest monsoon, El Niño, La Niña, Madden-Julian Oscillation, Indian Ocean Dipole, teleconnections, maritime operations, piracy | **15. NUMBER OF PAGES** 59 |
|---|---|
| | **16. PRICE CODE** |

| **17. SECURITY CLASSIFICATION OF REPORT** | **18. SECURITY CLASSIFICATION OF THIS PAGE** | **19. SECURITY CLASSIFICATION OF ABSTRACT** | **20. LIMITATION OF ABSTRACT** |
|---|---|---|---|
| Unclassified | Unclassified | Unclassified | UU |

NSN 7540-01-280-5500 Standard Form 298 (Rev. 2-89)
Prescribed by ANSI Std. 239-18

THIS PAGE INTENTIONALLY LEFT BLANK

**Approved for public release. Distribution is unlimited.**

**LONG-RANGE FORECASTING OF THE ONSET OF SOUTHWEST MONSOON WINDS AND WAVES NEAR THE HORN OF AFRICA**

Gary M. Vines
Lieutenant Commander, United States Navy
B.A., Thomas Edision University, 2007

Submitted in partial fulfillment of the
requirements for the degree of

**MASTER OF SCIENCE IN METEOROLOGY AND PHYSICAL OCEANOGRAPHY**

from the

**NAVAL POSTGRADUATE SCHOOL**
**December 2017**

Approved by: Tom Murphree
Thesis Advisor

Megan Hutchins
Fleet Numerical Meteorology and Oceanography Command,
Monterey, CA
Co-Advisor

Wendell Nuss
Chair, Department of Meteorology

THIS PAGE INTENTIONALLY LEFT BLANK

# ABSTRACT

The Asian southwest monsoon (SWM) east of the Horn of Africa (HOA) is important in planning and conducting maritime operations in this region. Skillful subseasonal to seasonal (S2S) forecasts of the SWM onset are needed for operational planning but are not yet available. We investigated the potential for S2S forecasting of the onset of SWM surface winds and ocean surface waves off HOA by analyzing global atmospheric and oceanic variables, and three onset states: early, normal, and late. We identified relationships between variables, precursor conditions for each state, and potential predictors for each state. We used the predictors to conduct 48 years of hindcasting. We assessed the skill of the hindcasts and identified two Pacific sea surface temperature (SST) predictors with a high potential to contribute to S2S forecasts of the onset. These results indicate that El Niño / La Niña (ENLN) variations are important in generating early, normal, and late onsets, but are not the only factors. The mechanisms that link remote SSTs to the onset appear to involve anomalous tropical Rossby-Kelvin waves that extend across the western tropical Pacific and the Indian Ocean–south Asian regions.

THIS PAGE INTENTIONALLY LEFT BLANK

# TABLE OF CONTENTS

# LIST OF FIGURES

# LIST OF TABLES

THIS PAGE INTENTIONALLY LEFT BLANK

# LIST OF ACRONYMS AND ABBREVIATIONS

| | |
|---|---|
| A | surface air temperature |
| ACAF | advanced climate analysis and forecasting |
| AN | above normal |
| AG | Arabian Gulf |
| AS | Arabian Sea |
| BN | below normal |
| BOM | Bureau of Meteorology (Australian) |
| C | total cloudiness fraction of the sky |
| CEFA | Climate, Ecosystem and Fire Applications |
| CFSR | Climate Forecast System Reanalysis |
| CFSRR | Climate Forecast System Reanalysis and Reforecast |
| CENTCOM | U.S. Central Command |
| CMF | Commander Maritime Forces |
| CPC | Climate Prediction Center |
| CSFR | Climate Forecast System Reanalysis |
| CTF | Combined Task Force |
| EN | El Niño |
| ENLN | El Niño/La Niña |
| ENSO | El Niño Southern Oscillation |
| ESRL | Earth System Research Laboratory |
| FNMOC | Fleet Numerical Meteorology and Oceanography Center |
| ft | feet |
| hPa | hecto-Pascal |
| HOA | Horn of Africa |
| IO | Indian Ocean |
| IOD | Indian Ocean Dipole |
| LL | low level |
| LRF | long-range forecast |
| LTM | long term mean |
| m | meters |

| | |
|---|---|
| mb | millibars |
| MEI | Multivariate ENSO Index |
| METOC | meteorology and oceanography |
| MJO | Madden-Julian Oscillation |
| m/s | meters per second |
| NASA | National Aeronautics and Space Administration |
| NAVCENT | Naval Forces U.S. Central Command |
| NCAR | National Center for Atmospheric Research |
| NCEI | National Center for Environmental Information |
| NCEP | National Centers for Environmental Prediction |
| NN | near normal |
| NOAA | National Oceanic and Atmospheric Administration |
| NPS | Naval Postgraduate School |
| NWIO | Northwest Indian Ocean |
| NWS | National Weather Service |
| PSD | Physical Sciences Division |
| RH | relative humidity |
| S2S | subseasonal to seasonal |
| SLOC | sea lines of communication |
| SLP | sea level pressure |
| SLPA | sea level pressure anomaly |
| SST | sea surface temperature |
| SSTA | sea surface temperature anomaly |
| SWH | significant wave height |
| SWHA | significant wave height anomaly |
| SWM | Southwest Monsoon |
| U | zonal component (of winds) |
| U.S.(A.) | United States (of America) |
| USCENTCOM | United States Central Command |
| V | meridional component (of winds) |
| WWIII | Wave Watch III |
| Z | geopotential height |

# ACKNOWLEDGMENTS

I am a Christian, meaning that I follow the beliefs and teachings of Jesus Christ from the New Testament books of the Bible and referenced to in the Old Testament books in the Bible. With no offense meant to anyone, it is a requirement of my faith that I acknowledge Christ before man, because it says in Matthew 10:32 (English Standard Version), “Everyone who acknowledges me publicly here on earth, I will also acknowledge before my Father in Heaven.” I want to be acknowledged. I believe that Jesus Christ is the son of God, born of a human mother (Mary), was crucified on the cross, rose again three days later and ascended to the right hand of God, which is why Jesus is referred to as a “living God.” I believe this was done to atone for the original sin brought into the world by Adam in the Garden of Eden, which separated God from mankind. I believe that Jesus’ sacrifice was an act of God getting closer to man, which is why Christianity is not a religion.

Thank you to my wife, Kathy, and my son, Jesiah. They sacrificed a lot of time away from me so I could do this. I’ll forever be grateful for that. I love both of them with all my heart and that is why I do this.

To Dr. Tom Murphree, your patience with me has been such a blessing.

To Mrs. Megan Hutchins, you inspired me to do a thesis on climatology. I really look up to you and I hope one day to garner as much clout in what I do as you have. Also, nice boots.

To my cohort: Jeffery Scooler, Chris Ayala, Alonzo Ingram, Larry Gulliver, Andy West, Aaron Morrone, and David Lorfeld. Many thanks. I couldn’t have done this without your help. May you all be blessed in your follow-on tours, and if you ever need anything and it is in my power to do so, consider it done. To Larry Gulliver, you were a friend to me like no other; may God bless you back times ten. To Chris Ayala, you truly inspire me.

My thesis research was a team effort and I acknowledged that fact when writing this thesis by using the terms *we* and *our* to describe the work done by the team.

THIS PAGE INTENTIONALLY LEFT BLANK

# I. INTRODUCTION

## A. MOTIVATION

Political instability in the Middle East has been ongoing. The U.S. military's increased presence in the Middle East (Kuwait, Bahrain, Iraq, Afghanistan, Pakistan, and sea lines of communications (SLOCs) into the Arabian Sea (AS) and Arabian Gulf (AG)), over the decades resulted in the establishment of the unified command, U.S. Central Command (CENTCOM), and its naval component, Naval Forces Central Command (NAVCENT) in 1983 (see Figure 1) (Schneller 2007; U.S. Central Command 2017; NAVCENT 2017). NAVCENT created the Combined Maritime Forces (CMF), which is a multi-national naval partnership, consisting of three combined task forces (CTF): CTF 150 (maritime security and counter-terrorism), CTF 151 (counter piracy) and CTF 152 (AG security and cooperation). The mission of the CMF is to promote security, stability and prosperity across approximately three million square miles of international waters, which includes some of the world's most important and busiest SLOCs (Figure 2; NAVCENT 2017). The SLOCs into and out of the Red Sea, Gulf of Aden, Indian Ocean (IO), and Gulf of Oman (Figure 2) are affected by the southwest monsoon (SWM) during the northern hemisphere summer. One of the most significant environmental impacts on maritime operations off the horn of Africa (HOA) are high winds and seas associated with the SWM. Feedback from fleet oceanographers, as well as formal inquiries from intelligence agencies who are invested in activity in this region, have indicated that a forecast of SWM winds and waves off the coast of HOA at long lead times (two weeks or longer) would be instrumental in their long-range planning.


Figure 1. Geopolitical depiction of all countries and waters within U.S. CENTCOM's area of responsibility. Source: CENTCOM (2017).

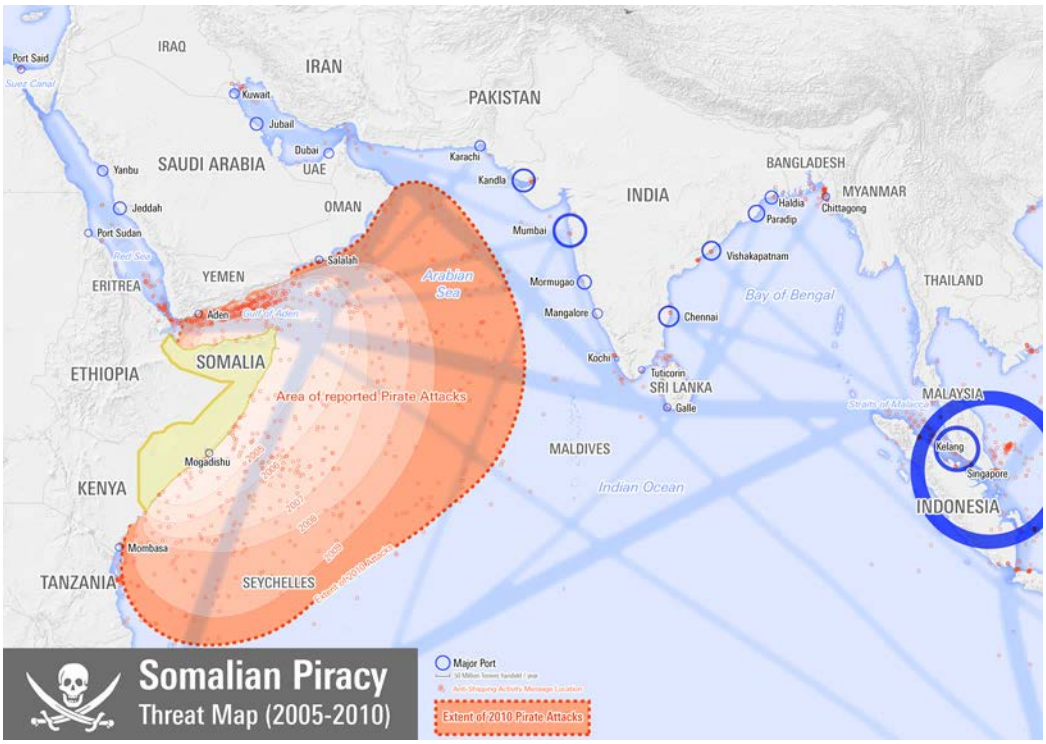


Figure 2. Sea lines of communication (blue lines) and piracy operations in 2005–2010 (orange shading and circles). Source: National Geospatial Intelligence Agency (NGA), (2010).

In June 2016, the climatology division at Fleet Numerical Meteorology and Oceanography Center (FNMOC) in Monterey, California, headed by Mrs. Megan Hutchins, received a request for information with regards to the onset of the SWM. Specifically, the question asked when the onset of surface winds and waves from the SWM, in the northwest Indian Ocean (NWIO) were expected. FNMOC collaborated with the Naval Postgraduate School (NPS) to find ways to improve long-range forecasts (LRF) of the SWM onset in the NWIO at 0 to 6 months lead times.

From the author's experience, military planners are aware of the general onset period of the SWM during the northern hemisphere summer, and many of the products used for long-range planning are often long-term mean (LTM) climatology products. LTM are multi-decadal means for specific meteorological and oceanography (METOC) variables. LTM products can be useful in long range planning, but climate variations, such as El Niño/La Niña (ENLN), can have impacts on the onset of the winds and seas

associated with the SWM and must be considered (Noska and Misra 2016; Ilczuk 2016; Chakraborty and Agrawal 2017; Murphree 2017d).

## B. PRIOR WORK

Much prior research had been done at NPS to increase the understanding of climate variations and improve long lead climate support to the fleet. The theses by LaJoie (2006) and Lemke (2010) focused specifically on the impacts of climate variations on military operations in HOA. LaJoie (2006) explored seasonal precipitation in the HOA during ENLN. Lemke (2010) developed and tested methods for LRF of precipitation variations in HOA. He also identified several remote predictors (a predictor is a variable that helps predict for the predictand), teleconnections (which are linkages between environmental conditions occurring in widely separated regions of the globe), and intraseasonal to interannual climate variations that affect HOA precipitation (Lemke 2010; Chakraborty and Agrawal 2017; Murphree 2017a-d. The results from Lemke (2010) and other studies indicate that accurate LRFs of precipitation in and near HOA are possible. However, we were not able to find comparable studies of long range forecasting of the winds and waves in the maritime region offshore of HOA. Ilczuk (2016) identified intraseasonal to interannual climate variations and teleconnections that affect the NWIO and southwest Asian regions, but did not specifically address the long range forecasting of SWM winds and waves offshore of HOA.

A number of prior studies have investigated the onset of the SWM precipitation over south Asia. For example, Singh and Goyal (1997) attempted to forecast the onset of the SWM precipitation over Delhi, India based on air temperatures and winds at 850–10 hecto-Pascals (hPa). Webster, et al. (1998), Kumar (2004), Oo (2007); and Karmakar (2015) investigated how intraseasonal to interannual climate variations can affect the arrival date of SWM precipitation in South Asia.

The U.S. National Weather Service (NWS) provides forecasts of winds and seas out to 180 hours for the IO. These forecasts are available at: http://polar.ncep.noaa.gov/waves/viewer.shtml?-multi_1-latest-indian_o-u10-.

The Climate, Ecosystem and Fire Applications (CEFA) website (https://cefa.dri.edu/CFS/cfs.php) provides global scale forecasts out to four months of mean and anomalous 500 millibar (mb) geopotential heights (Z); 850 mb Z, relative humidity (RH), and temperature; 500 mb RH; 200 mb winds and heights; and 300 mb Z and winds. The forecasts are based on CFSv2 forecasts from the U.S. National Centers for Environmental Prediction (NCEP; Saha et al. 2014).

The U.S. National Weather Service (NWS) Climate Prediction Center (CPC) has an East Africa Weather and Climate webpage (http://www.cpc.ncep.noaa.gov/products/international/nmme/nmme_seasonal_body.html) that provides seasonal forecasts out to 180 days for air temperature, precipitation, and sea surface temperature (SST). However, operational subseasonal to seasonal (S2S) forecasts the maritime region off HOA are very limited, especially for ocean surface waves, and at the temporal and spatial resolution desired by operational planners.

## C. OVERVIEW OF THIS STUDY

Surface winds and seas offshore HOA during the SWM have significant operational impacts on the U.S. Navy, so we focused on investigating the potential for skillful S2S forecasting of these variables. Based on the author's experience and requests received by the climatology division of FNMOC, operational S2S forecasts of the SWM would be very useful to military planners and operational METOC officers to support planning and recommendations to leadership.

We focused our research on the following questions,

1. At S2S lead times (two weeks to nine months), how can we forecast the onset of the SWM over the NWIO?
2. Specifically, how can we forecast when the surface winds and waves will ramp up with the monsoon? Will it begin sooner or later than the normal onset?
3. What climate variations and teleconnections can explain early and late onsets of the SWM?
4. What predictors can help us forecast early and late onsets at S2S lead times?

## D. THESIS ORGANIZATION

Chapter I discusses our motivation and prior work on the SWM, and gives an overview of our thesis. Chapter II focuses on the data sets, variables, and methods that we used, including predictand selection, conditional composites, correlations, predictor selection, tercile matching, hindcasting, and the steps we took for each of these methods. Chapter III provides our main results and findings. Chapter IV provides a summary of our results and recommendations for future research.

# II. DATA AND METHODS

## A. FOCUS REGION

Our focus region was the maritime region off the coast of the HOA, but we also investigated the entire IO, which is shown in Figure 3. In searching for teleconnections, we also focused on the Indo-Pacific region and the Maritime Continent shown in Figure 4. We also researched the entire globe to analyze the processes that affected our focus region, and to identify potential predictors.

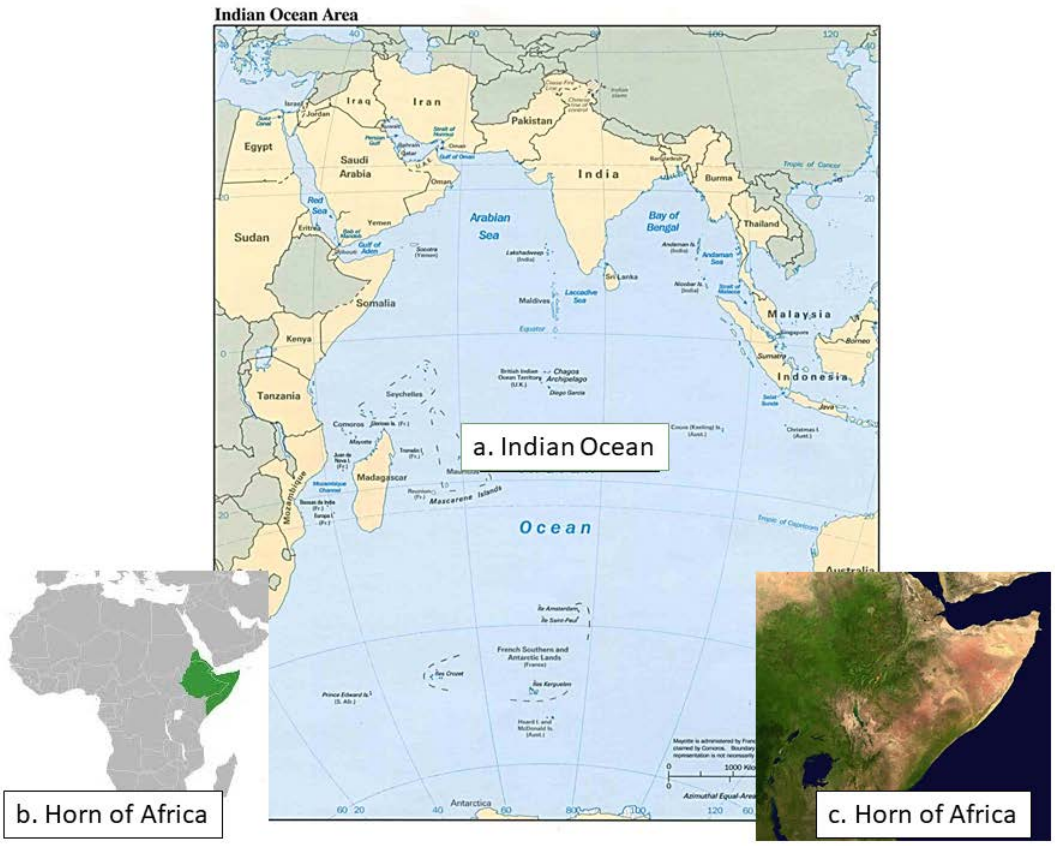


Figure 3. The Indian Ocean region with insets that show the location of the Horn of Africa (HOA). Adapted from: (a) University of Texas at Austin (2017), (b and c) Wikimedia Commons (2017).

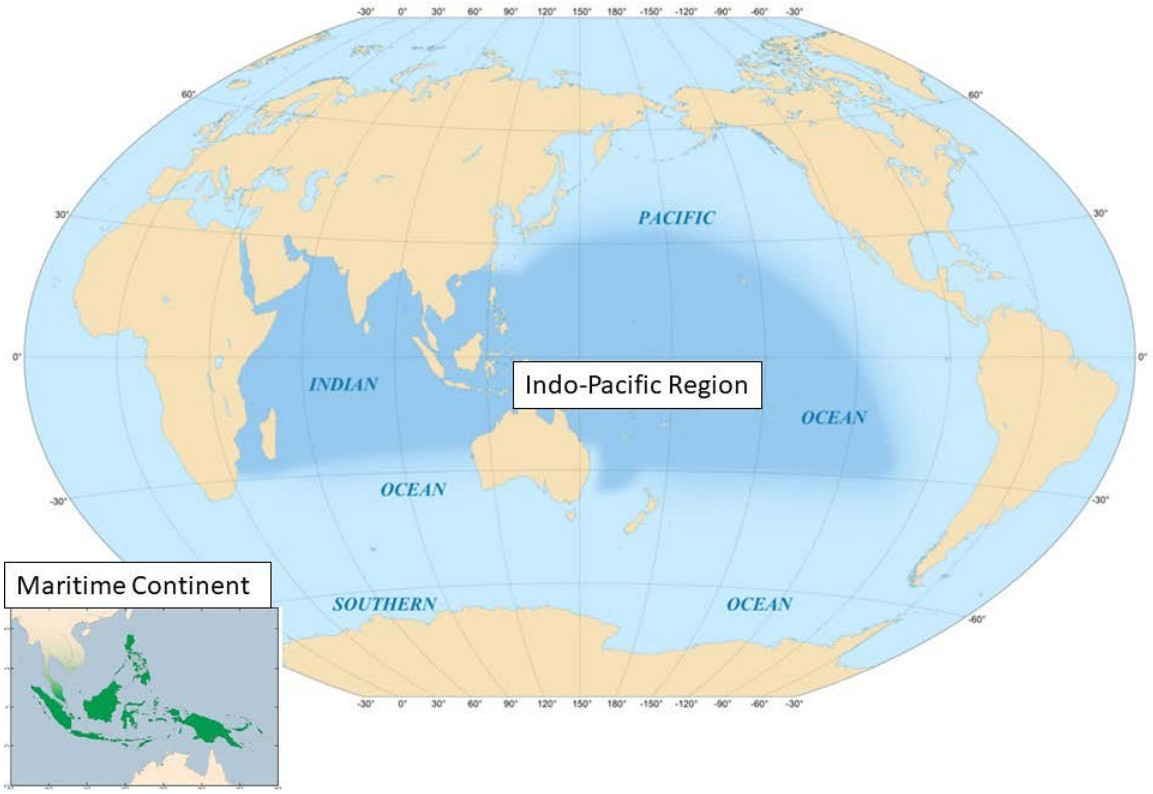


Figure 4. The Indo-Pacific region of the world, where most of our analysis was focused. The Maritime Continent is shown in the inset. Sources: Wikipedia (2017) and BOM (2017).

## B. DATA

### 1. NCEP/NCAR Reanalysis Data Set

The main data we used was monthly mean data from the National Centers for Environmental Prediction (NCEP) / National Center for Atmospheric Research (NCAR) reanalysis, often referred to as the R1 dataset (Kalnay et al. 1996; Kistler et al. 2001). R1 is a multi-decadal global reanalysis data set spanning 1948–present. For our study, we chose the years 1970–2017 because this period provided several decades of data and focused on the period in which satellite data has steadily become more abundant. Our LTM products were based on data from 1981–2010. The R1 data is available at a 2.5 degree horizontal resolution. More information about the R1 data set can be found in

Kalnay et al. (1996). We did much of our analysis of the R1 data via the analysis and plotting sites provided by the National Oceanic and Atmospheric Administration (NOAA) Earth Systems Research Laboratory (ESRL) Physical Sciences Division (PSD). We used the ESRL PSD time series website (https://www.esrl.noaa.gov/psd/data/timeseries/) to download time series of R1 variables in both graphical and tabular form. The graphics show the variations in the monthly averaged variables. The tabular form simply lists the date and the value of the variable selected from 1948 until the present. The time series were vital to this thesis in that they could be adapted and uploaded to the ESRL correlation website (https://www.esrl.noaa.gov/psd/data/correlation/), as a "custom correlation." We primarily used these websites to build our time series and create correlation maps for investigating potential predictor-predictand relationships. We also used other ESRL PSD websites to create conditional composite maps and other figures. All figures that show R1 data were created at the ESRL sites.

### 2. NOAA Wavewatch III (WWIII) Data Set

We used monthly mean data from phase 1 of the NOAA Wavewatch III (WWIII) reanalysis hindcast data set to describe ocean surface waves (NOAA/NWS 2017a, b). This data set has 17 regular latitude-longitude grids, and the NCEP Climate Forecast System Reanalysis and Reforecast (CFSRR) homogeneous dataset of hourly high-resolution winds (NOAA/NWS 2017a, b). We accessed this ocean surface wave data via the FNMOC Advanced Climate Analysis and Forecasting (ACAF) site. All figures that show this wave data were created at the ACAF site.

## C. VARIABLES

The main variables that we analyzed were: SST and SST anomalies (SSTA) in degrees Celsius, meridional winds (V) at 1000 mb in meters per second (m/s), significant wave height (SWH) in feet (ft), sea level pressure (SLP) in millibars (mb), and geopotential height (Z) at 1000 mb, 850 mb and 200 mb in geopotential meters. The main climate indices that we referenced during our research were: (a) the Multivariate El Niño-Southern Oscillation Index (MEI), an index based on tropical Pacific SLP, V and U components of surface winds, SST, surface air temperature (A), and total cloudiness

fraction of the sky (C) (Wolter 2011); and (b) the Nino 3.4 index of tropical Pacific SSTA in the area bounded by 5°N-5°S, 120°W-170°W (Figure 5).

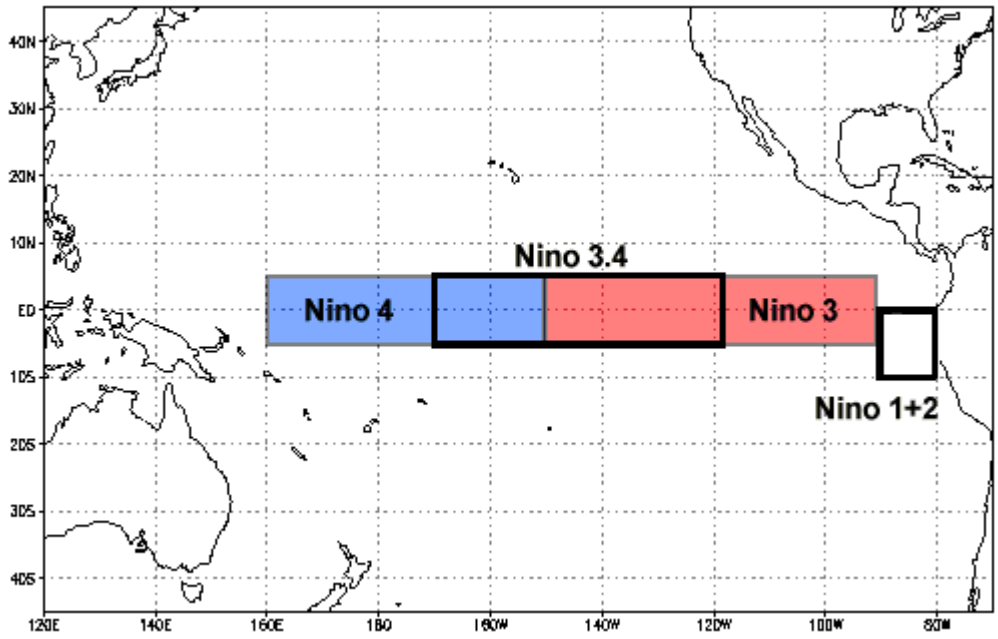


Figure 5. The Nino 3.4 area in the tropical Pacific. Source: NOAA/NCEI (2017)

## D. ANALYSIS AND FORECAST METHODS

### 1. Predictand Selection

We chose as our initial predictand the 1000 mb winds over the ocean near HOA in May because: (a) May is the month in which early and late onsets of the SWM tend to become apparent; (b) the SWM winds are especially strong in this region; (c) these winds are important in generating the corresponding ocean surface waves in this region; and (d) these winds and associated waves are important to U.S. Navy operations in this region. The meridional (V) component of these winds is the dominant component of the SWM winds in this region, so we chose V in May off HOA as our predictand variable. We used conditional compositing of V in the ten years with the earliest onsets and in the ten years with the latest onsets to identify a specific predictand location. This location was in the maritime region off HOA for which we found the largest variations in V, the largest

anomalies in V, and the most opposite anomalies in V, when we compared the early and late composites. We identified an early (late) onset occurring when the predictand V anomaly in May had a large positive (negative) value in the upper (lower) tercile of all values for our 1970–2017 study period.

### 2. Conditional Composite Analysis

A long term mean (LTM) is the average over many years, usually 30 or more years. A conditional composite mean is an average of only specific years that meet a specific condition, such as years in which an El Niño (EN) occurred. In our case, we calculated the conditional composite means for early and late onset SWM years, and subtracted from those conditional composite means the corresponding LTMs to calculate the conditional composite anomalies for early and late onsets. The ESRL and FNMOC's ACAF websites, have the ability to readily calculate anomalies. We analyzed conditional composites for ten early onset years and ten late onset years for the predictand V and predictand V anomaly, SLP, SLP anomaly (SLPA), vector winds, vector wind anomaly, SST and SST anomaly (SSTA). We also assessed the mechanisms, teleconnections, wave trains, and other relationships indicated by the conditional composite anomalies to infer the climate system mechanisms that led to the anomalies and the early and late onsets.

### 3. Correlation Analysis

After we found our predictand V, we used the correlations section of the ESRL website (https://www.esrl.noaa.gov/psd/data/correlation/) to search for potential predictors. To analyze the potential for predictors, and to discover potential climate mechanisms that might explain the correlations, we correlated a number of variables, including: predictand V with global SSTs, global V winds with global SSTs, and global V winds with global MEI (Table 1). We calculated correlations with one variable lagging the other variable by zero months to six months. We focused our assessments of the correlation maps, and our search for potential predictors, on regions in which the correlations were large in magnitude, extended over large areas, and were persistent during all lead times.

Table 1. Table of correlation experiments conducted to search for potential predictors and to investigate dynamical processes.

| Correlation Experiments | | | |
|---|---|---|---|
| **Experiment Number** | **Variable 1** | **Variable 2** | **Variable 2 Leading by** |
| **1** | **May predictand V winds** | **Global SST** | **0-6 months** |
| **2** | **Global V winds** | **Global MEI** | **0-6 months** |
| **4** | **May Global V Winds** | **Global SST** | **0-6 months** |
| **5** | **May U winds** | **Nino 3.4** | **0-6 months** |
| **6** | **Z850** | **Nino 3.4** | **0-6 months** |
| **7** | **Z850** | **SST in NWIO** | **0-6 months** |
| **8** | **May predictand V winds** | **Global V winds** | **0-6 months** |

For the 48 years in our study period (1970-2017), correlations with magnitudes greater than 0.24 are statistically significant at the 95% confidence interval, based on the standard normal distribution of a two-tailed test (Wilks 2006; NOAA/ESRL 2017).

## 4. Predictor Selection

We used the correlation results to identify potential predictors, using the criteria described in the preceding section. In particular, we identified potential predictors as variables for which the correlations with the predictand V showed regions in which the correlations were large in magnitude, extended over large areas, and were persistent during all lead times.

### 5. Tercile Matching Method for Hindcasts

We ranked the 48 years of our study period according to the value of the V predictand in May of each year. We labeled the upper tercile of those years, in which the V magnitude was greatest, as the above normal (AN) years, the middle tercile as the near normal (NN) years, and the lowest tercile as the below normal (BN) years. We used these predictand terciles as our forecast targets. That is, we attempted in our hindcasts to correctly forecast the tercile in which the V predictand would occur for each year in the study period. Our hindcasts were based on tercile matching, in which the predictand tercile for each year was compared, or matched, with the corresponding predictand tercile to determine the forecast. For a predictor that was positively (negatively) correlated with the predictand, we counted a forecast for a given year as a hit if the predictor and predictand were in the same (opposite) tercile for that year.

We conducted a tercile matching hindcast for each year for each predictor-predictand pair. We assessed the skill of each predictor by calculating the hit rate for the hindcasts generated using that predictor. The hit rate is the ratio of correct forecasts of an event (AN, NN, or BN) to the number of times the event occurred:

$$Hit\ rate = \ H = A/(A + C)$$

where A = number of correct forecasts of the event, C = number of missed forecasts of the event (Wilks 2006). The hit rate is shown in percentage.

## E. SUMMARY OF CLIMATE ANALYSIS AND LONG-RANGE FORECAST METHODOLOGY

Prior theses from Heidt (2006) and Lemke (2010) used methods similar to ours and to those described in Wilks (2006). We used conditional composite analyses to select our predictand, compare early and late onset years for a range of variables, identify dynamical processes, correlate a range of variables, and identify potential predictors based on the correlation results. We divided our predictand and potential predictors into terciles, and then compared them in a series of hindcasts to determine their skill in predicting early, normal, and late onsets at subseasonal to seasonal (S2S) lead times.

THIS PAGE INTENTIONALLY LEFT BLANK

# III. RESULTS

## A. PREDICTAND SELECTION

The focus of our study was on S2S forecasting of the onset of the onset of SWM surface winds and ocean surface waves off HOA. Thus, we chose the 1000 mb winds off HOA in May as our initial predictand. We compared the zonal and meridional components of those winds and determined that the meridional component, V, tended to be stronger than the zonal component U. So we selected V as the component to use for our predictand.

We then constructed a time series of V off HOA for our 48 year study period, 1970–2017. We divided the 48 years of V data into above normal (AN), near normal (NN), and below normal (BN) terciles. We used the AN years to represent early onset years, the NN years to represent normal onset years, and the BN years to represent late onset years.

We also composited data for V and other variables for the ten years with the highest V values (1978, 1990, 1999, 2000, 2001, 2002, 2004, 2006, 2008 2011) and the lowest V values (1972, 1982, 1987, 1991, 1992, 1993, 1998, 2005, 2014, 2015). We used the high ten composite to characterize early onsets and the low ten composite to characterize late onsets. We created maps of the V anomalies during the early ten years and the late ten years. From these maps, we identified a region off HOA in which the V anomalies were large in both the early years and late years. This region is located at 02N-14N, 52E-67E. We selected this region as the predictand region for our study. Thus, our predictand was May V winds at 1000 mb within a box located at 02N-14N, 52E-67E. For brevity, we refer to this as the predictand V. Figures 6 and 7 show the predictand V time series for 1970–2017, along with the highest ten and lowest ten years, and the three terciles previously described.

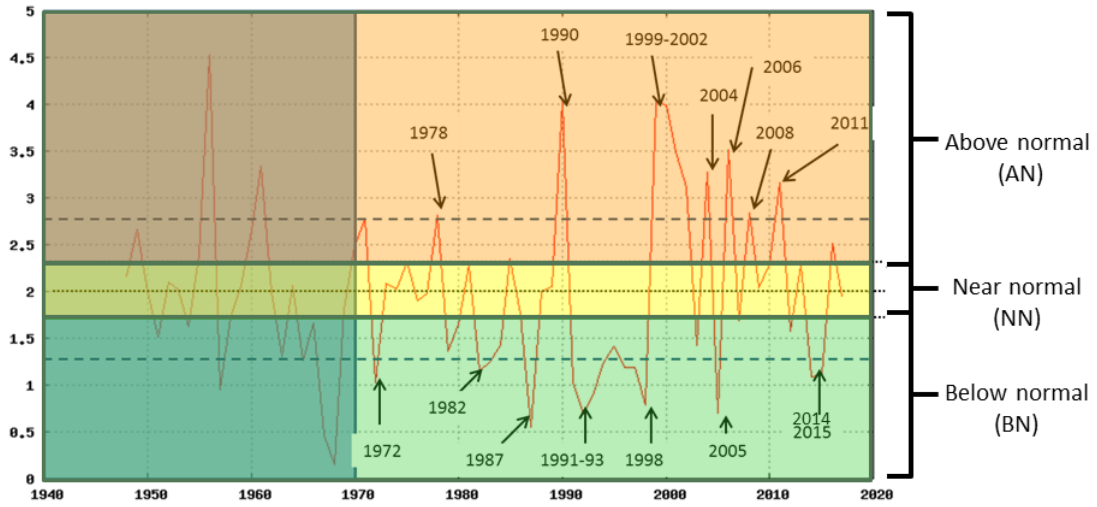


Figure 6. Predictand V time series for 1970–2017. Highlighting: above normal years: peach; near normal years: yellow; below normal years: light green. Years before 1970 are shaded grey because our research focused on 1970–2017.

| Above Normal (early onset) | | Near Normal (normal onset) | | Below Normal (late onset) | |
|---|---|---|---|---|---|
| Year | v (m/s) | Year | v (m/s) | Year | v (m/s) |
| 1990 | 4.038 | 1981 | 2.289 | 1995 | 1.412 |
| 1999 | 4.038 | 2013 | 2.288 | 1979 | 1.358 |
| 2000 | 3.992 | 1973 | 2.051 | 1983 | 1.245 |
| 2006 | 3.507 | 1989 | 2.037 | 1994 | 1.239 |
| 2001 | 3.492 | 2009 | 2.02 | 1996 | 1.193 |
| 2004 | 3.273 | 1974 | 2.006 | 1997 | 1.186 |
| 2011 | 3.159 | 1988 | 1.978 | 1982 | 1.156 |
| 2002 | 3.107 | 1977 | 1.951 | 2015 | 1.110 |
| 2008 | 2.833 | 2017 | 1.905 | 2014 | 1.092 |
| 1978 | 2.813 | 1976 | 1.767 | 1972 | 1.031 |
| 1971 | 2.778 | 1986 | 1.688 | 1991 | 1.023 |
| 2016 | 2.511 | 2007 | 1.655 | 1993 | 0.891 |
| 1970 | 2.474 | 1980 | 1.578 | 1998 | 0.786 |
| 1985 | 2.356 | 2012 | 1.521 | 2005 | 0.700 |
| 1975 | 2.315 | 2003 | 1.427 | 1992 | 0.685 |
| 2010 | 2.292 | 1984 | 1.423 | 1987 | 0.547 |

10 strongest years

10 weakest years

Figure 7. Predictand V values for 1970–2017 binned into above normal, near normal, and below normal terciles (left/peach column, middle/yellow column, and right/green column, respectively), corresponding to early, normal, and late onset years. The ten years with the highest (lowest) V predictand values are marked by a blue (red) box.

## B. CONDITIONAL COMPOSITE ANALYSIS

### 1. SLPA

In our conditional composite analyses, we first analyzed SLP. We did this in part to determine how the south Asian low, the Mascarene High, and other features of the SLP field in May might be related to early and late onsets. Figure 8 shows the LTM SLP in May, with the south Asian low centered over India and the Mascarene High centered over the south Indian Ocean. Tropospheric warming contributes to the south Asian low and tropospheric cooling to the Mascarene High (e.g., Hastenrath 1985). Lower tropospheric air tends to flow counterclockwise around the Mascarene High, then across the equator, and then counterclockwise into the south Asian low. Topographic forcing along the east coast of Africa helps to concentrate the flow near the coast and create the Somali Jet (e.g., Hastenrath 1985).

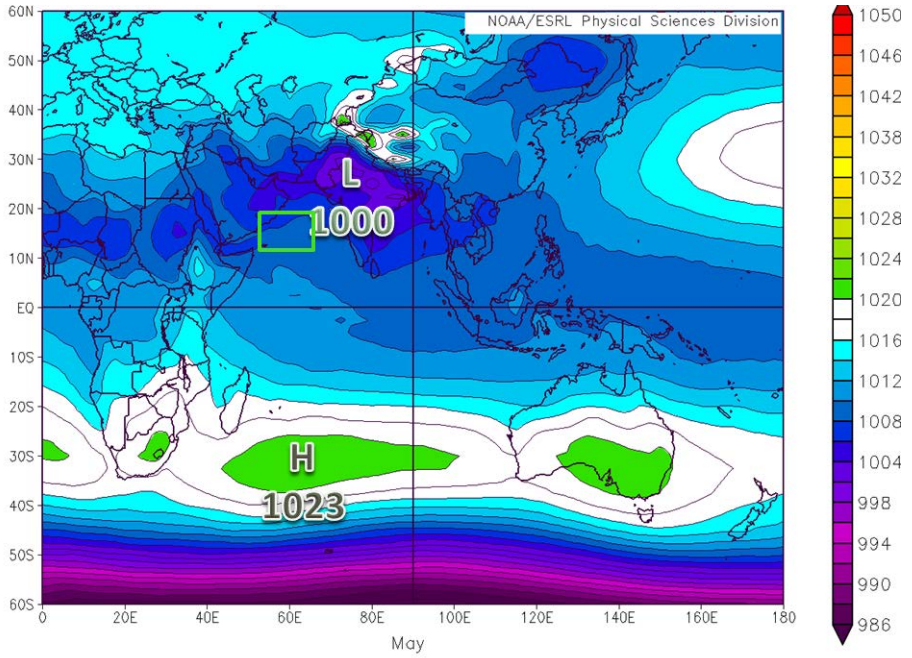


Figure 8. LTM sea level pressure (mb) in May. The predictand V location is shown by the green box off HOA.

Figures 9 and 10 show the composite SLPA in May for the early and late onset years. During the early (late) years, the south Asian low was anomalously negative (positive), consistent with an anomalously strong (weak) flow off HOA into that low. Thus, the Asian low anomalies were opposite for the early and late onset years. However, Figures 9 and 10 show that the SLPAs for the Mascarene High region were not clearly opposite for the early and late onset years. This indicates that anomalies in the south Asian low may have been more important than anomalies in the Mascarene High in creating early and late onsets (cf. Singh and Goyal 1998). The negative south Asian anomalies in the early onset case were part of a larger pattern of anomalies that extends west-northwestward and southwestward from the maritime continent (Figure 9), a pattern that is consistent with an anomalous tropical Rossby-Kelvin wave response to *positive* SST and *positive* tropospheric convection anomalies in the maritime continent (MC) region (Figure 9; cf. Gill 1982). Similarly, the positive south Asian anomalies in the late onset case were part of a bigger pattern of anomalies that extends west-northwestward and southwestward from the (Figure 10), a pattern that is consistent with an anomalous tropical Rossby-Kelvin wave response to *negative* SST and *negative* tropospheric convection anomalies in the MC region (Figure 10). This suggests that: (a) both the early and late onsets may be associated with climate variations that involve SST and convection anomalies near the MC— such as El Niño / La Niña (ENLN), Madden-Julian Oscillation (MJO), and Indian Ocean Dipole (IOD); and (b) teleconnections between the HOA region and MC are important in creating early and late onsets.

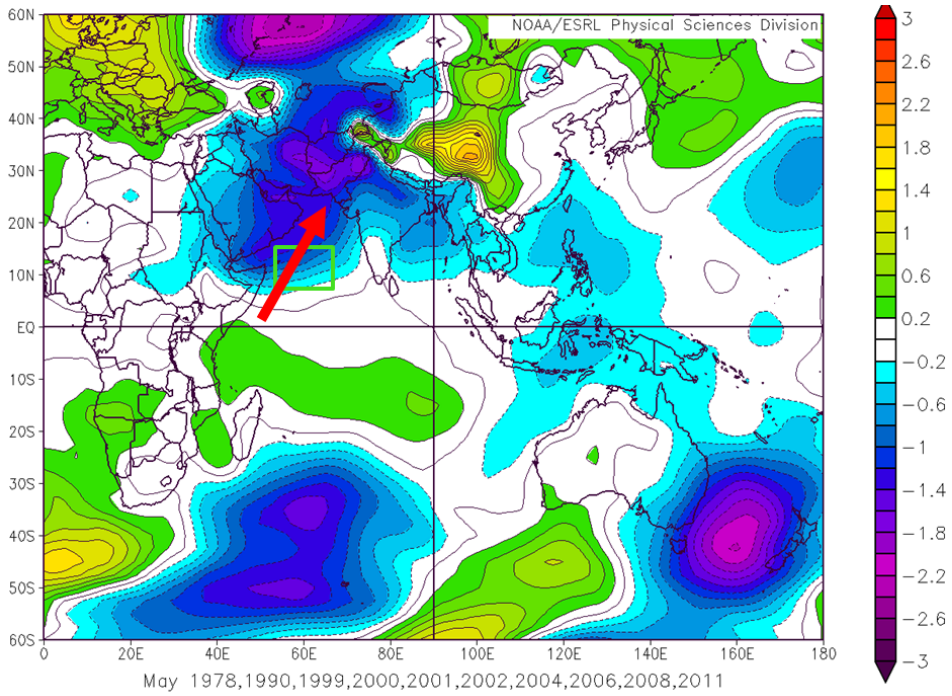


Figure 9. Sea level pressure anomalies (mb) in May during early onset years. The predictand V location is shown by the green box off HOA. The red arrow indicates anomalously strong SWM winds off HOA inferred from the anomalous SLP gradients in the western IO region.

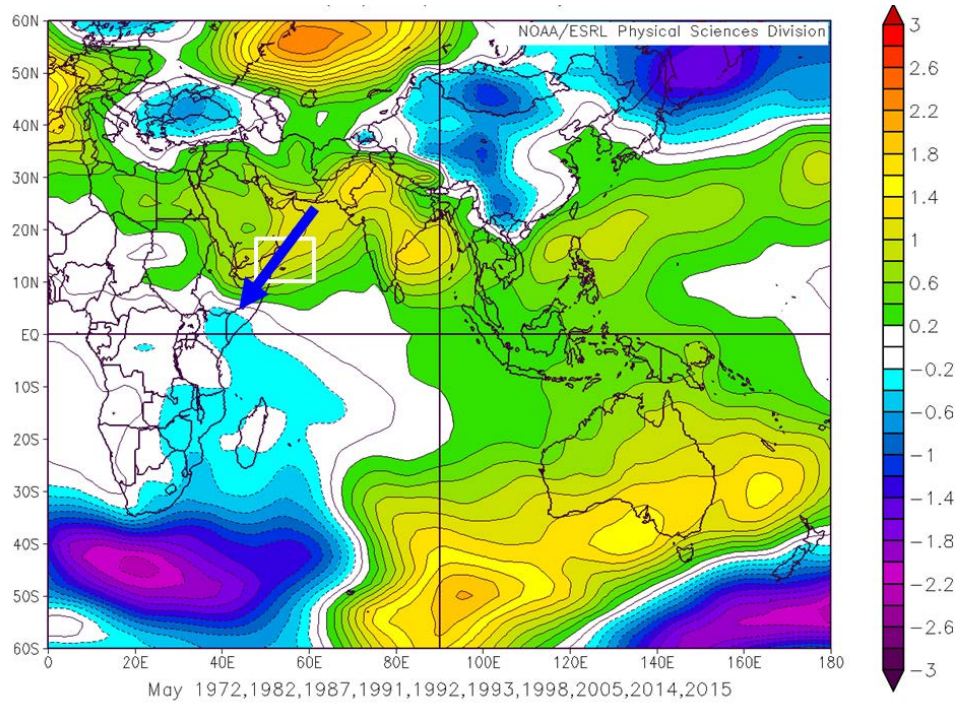


Figure 10. Sea level pressure anomalies (mb) in May during late onset years. The predictand V location is shown by the white box off HOA. The blue arrow indicates anomalously weak SWM winds off HOA inferred from the anomalous SLP gradients in the western IO region.

### 2. 1000 MB Vector Wind Anomalies

The 1000 mb vector wind anomalies (Figures 11–12) were northeastward (southwestward) in the northwest IO (NWIO) in the early (late) onset years. The wind anomalies correspond to stronger (weaker) than normal wind speeds in this region (not shown). The wind anomalies are consistent with the SLPAs (Figures 9–10) and with anomalous onshore advection of warm moist air from the tropical IO into India. This advection would favor tropospheric convection over India, while the late onset wind anomalies would disfavor that advection and convection.

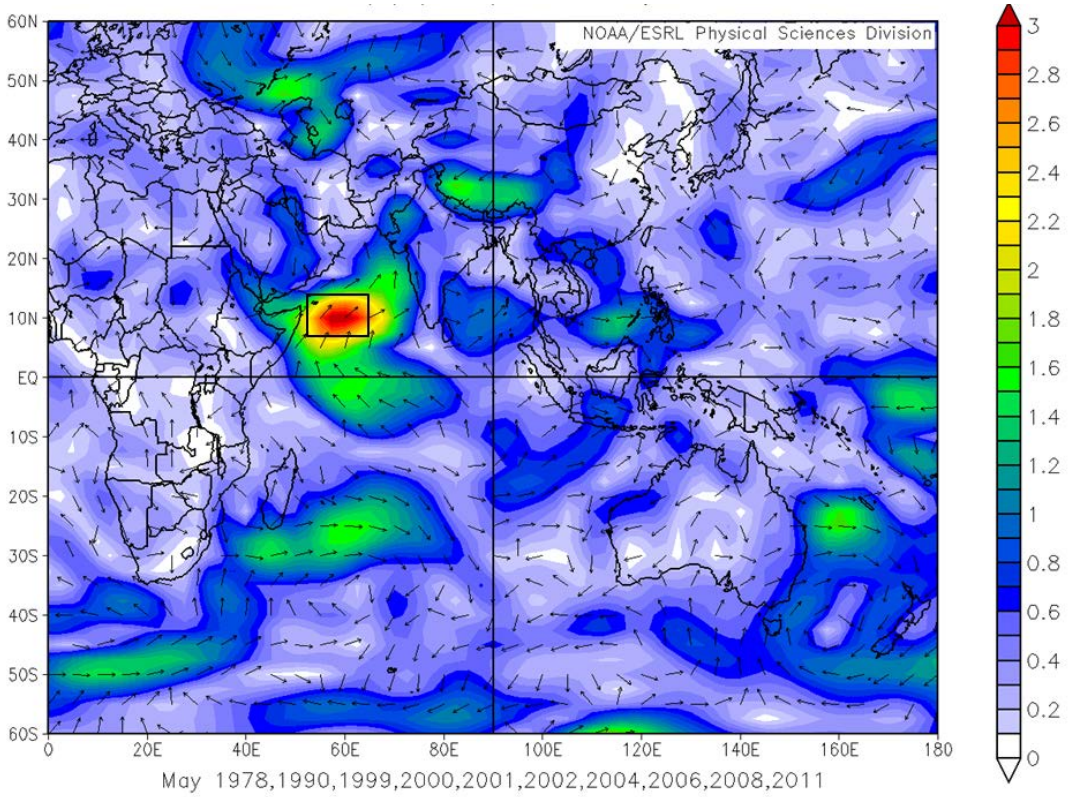


Figure 11. Vector wind anomalies (m/s) in May during early onset years. The predictand V location is shown by the black box off HOA.

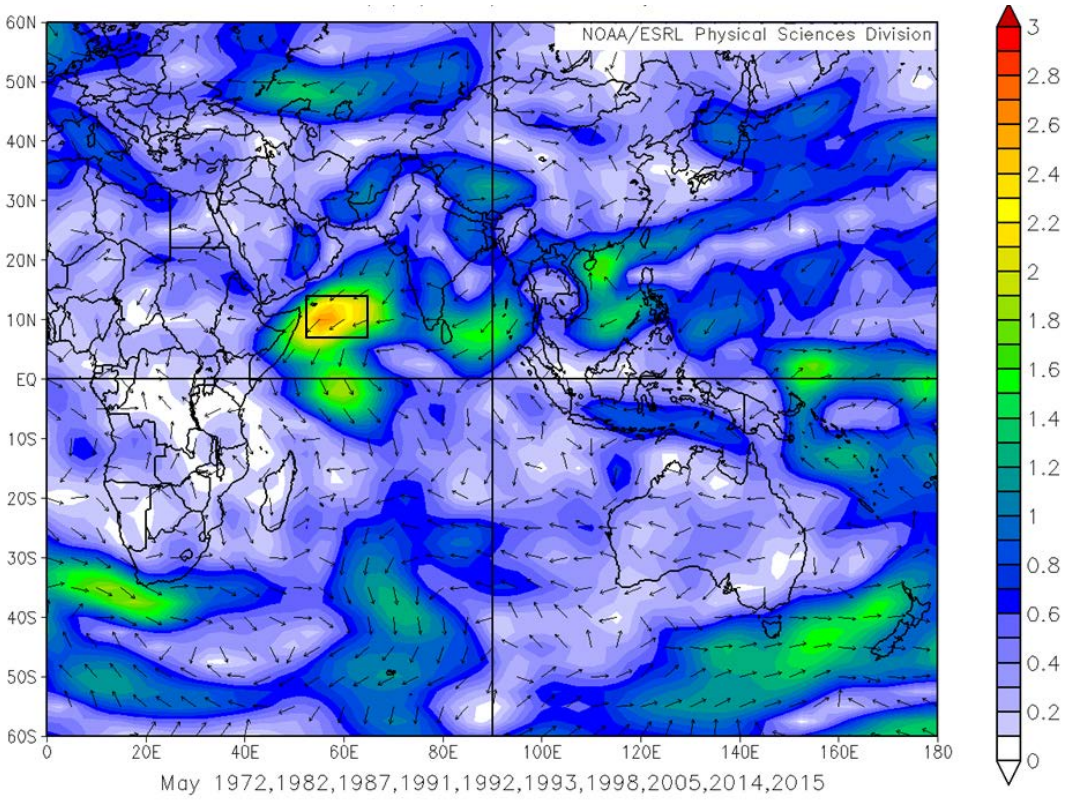


Figure 12. Vector wind anomalies (m/s) for May during late onset years. The predictand V location is shown by the black box off HOA.

### 3. SWH Anomalies

The significant wave height (SWH) anomalies (Figure 13) were positive (negative) in the NWIO in the early (late) onset years, consistent with the vector wind anomalies (Figures 11–12). The wave direction anomalies (not shown) were northeastward (southwestward) in the early (late) onset wind anomalies, which is also consistent with the vector wind anomalies.

Thus, the SLP, vector wind, and SWH anomalies (Figures 9–14) are all consistent with the expectation that early (late) onset years are associated with stronger (weaker) than normal northeastward monsoon flow and higher (lower) than normal ocean surface waves in the NWIO.

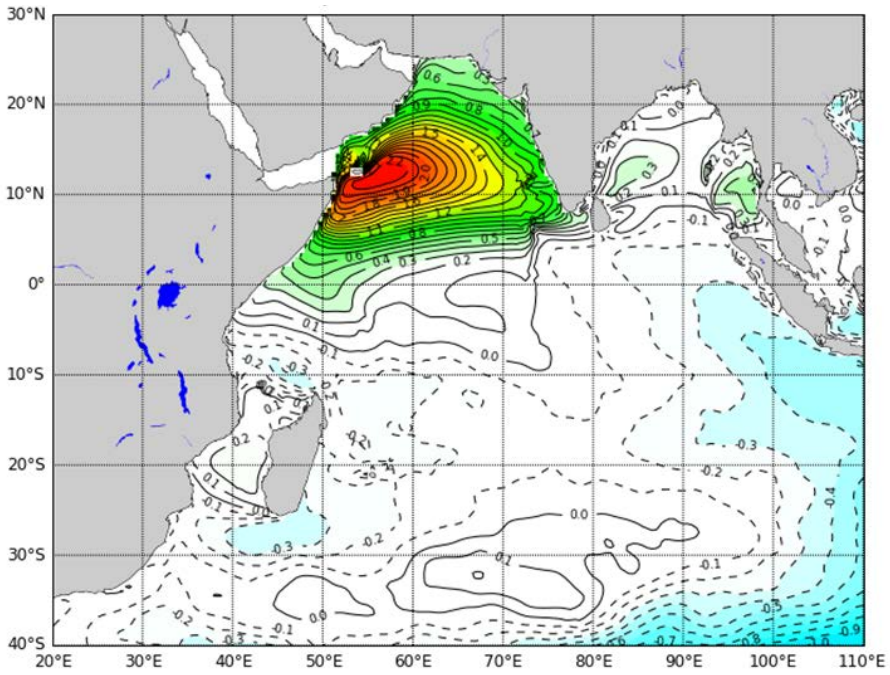


Figure 13. SWH anomalies (ft) for May during early onset years

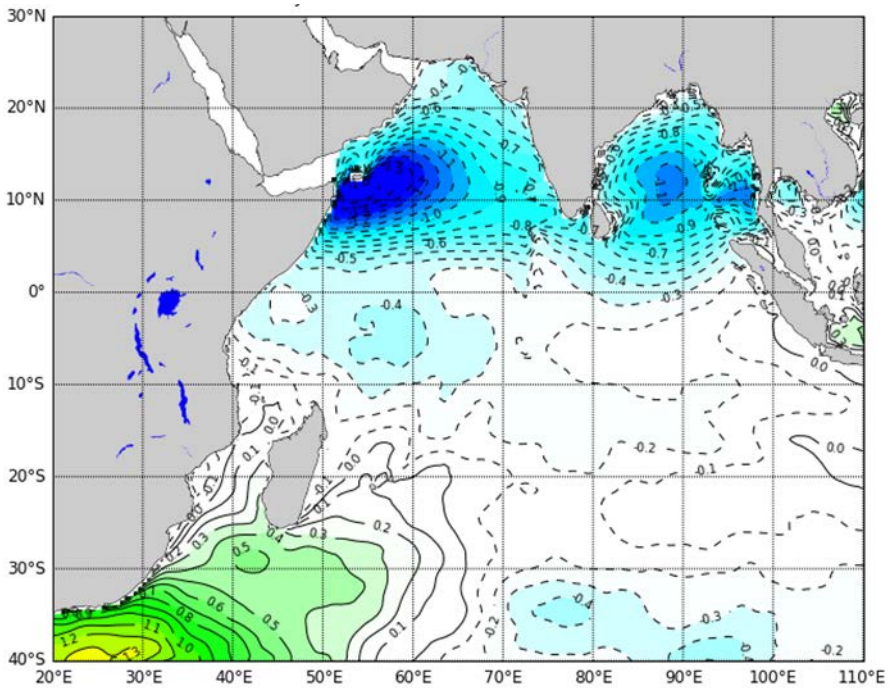


Figure 14. SWH anomalies (ft) for May during late onset years.

## 4. Z850 Anomalies

Figures 15–16 show the composite Z850 anomalies in May for the early and late onset years. These Z850 results are consistent with the SLPAs in showing: (a) negative (positive) anomalies during the early (late) years over south Asia; and (b) anomalies in the Mascarene High region that were not clearly opposite for the early and late onset years. This indicates that anomalies over south Asia may have been more important than anomalies in the Mascarene High in creating early and late onsets. The negative south Asian anomalies in the early onset case were part of a larger pattern of anomalies that extends west-northwestward and southwestward from the maritime continent (Figure 15), a pattern that is consistent with an anomalous tropical Rossby-Kelvin wave response to *positive* SST and *positive* tropospheric convection anomalies in the maritime continent (MC) region (cf. Gill 1982). Similarly, the positive south Asian anomalies in the late onset case were part of a bigger pattern of anomalies that extends west-northwestward and southwestward from the (Figure 16), a pattern that is consistent with an anomalous tropical Rossby-Kelvin wave response to *negative* SST and *negative* tropospheric convection anomalies in the MC region. This suggests that: (a) both the early and late onsets may be associated with climate variations that involve SST and convection anomalies near the MC—such as El Niño / La Niña (ENLN), Madden-Julian Oscillation (MJO), and Indian Ocean Dipole (IOD); and (b) teleconnections between the HOA region and MC are important in creating early and late onsets. The negative (positive) Z850 anomalies over south Asia in the early (late) onset years indicate enhanced (suppressed) tropospheric convection in that region, consistent with the temperature and moisture advection anomalies implied by the vector wind anomalies (Figures 11–12).

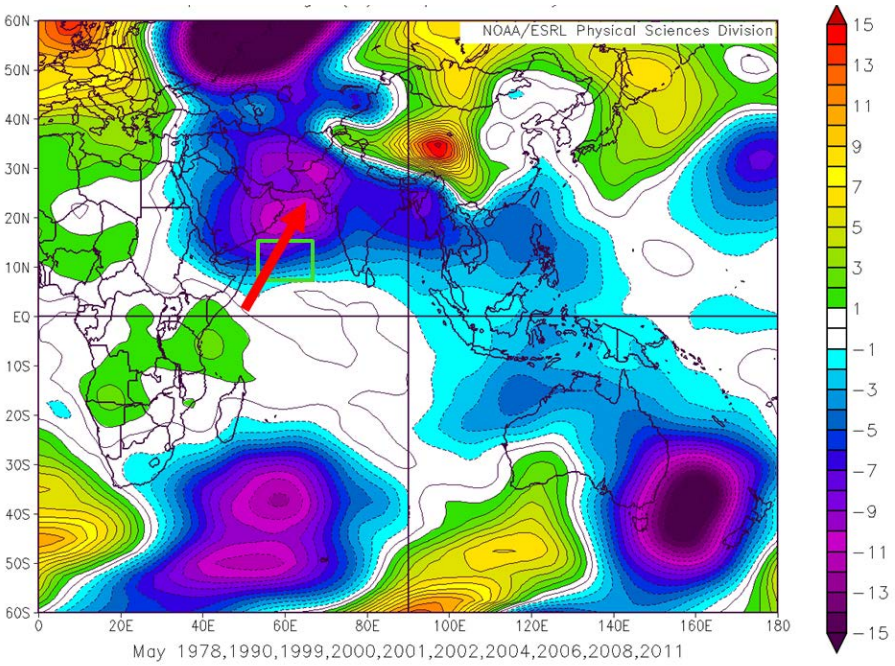


Figure 15. 850 mb geopotential height anomalies (Z850, m) in May during early onset years.

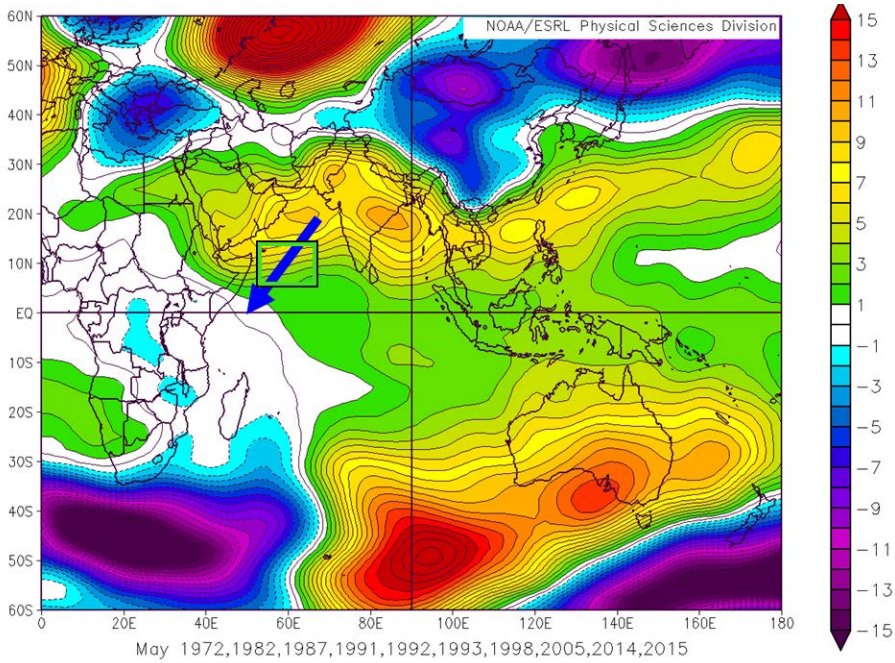


Figure 16. 850 mb geopotential height anomalies (Z850, m) in May during late onset years.

## 5. Z200 Anomalies

Figures 17–18 show the composite Z200 anomalies in May for the early and late onset years. Note the positive (negative) anomaly over south Asia in the early (late) composite, which is consistent with the idea that the early (late) years are associated with anomalously strong (weak) tropospheric convection over south Asia. The Z200 anomaly results also show alternating positive and negative anomalies in the northern midlatitudes that indicate an anomalous zonal Rossby wave train in this region. The alternating positive and negative anomaly patterns are roughly opposite between the early and late onset composites, and are clearer in the early onset composite. The Z200 anomalies also show symmetry about the equator and structures along the equator that are consistent with an anomalous tropical Rossby-Kelvin wave response to anomalous tropospheric convection near the MC (cf. Gill 1982).

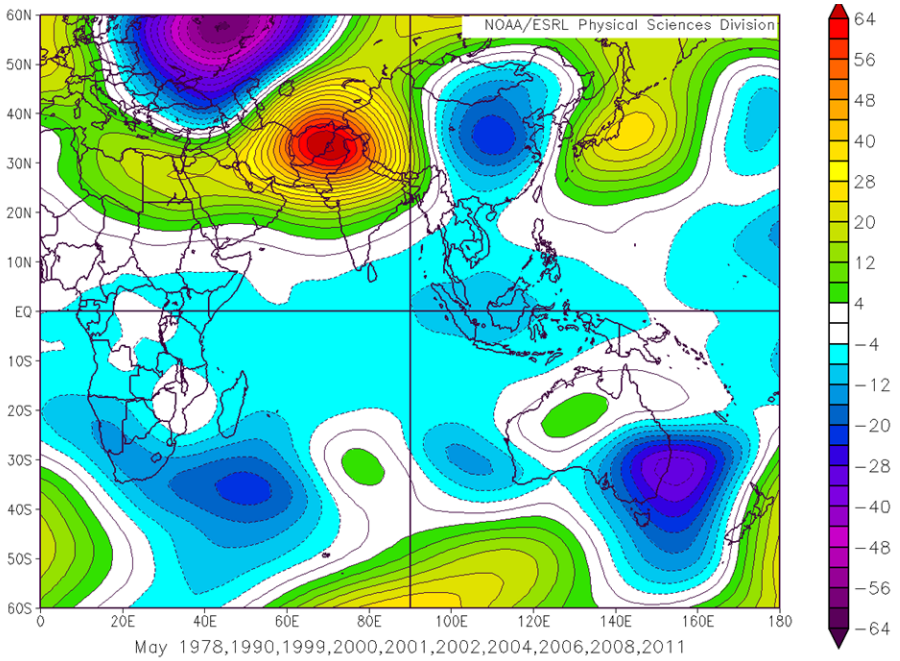


Figure 17. 200 mb geopotential height anomalies (Z200, m) in May during early onset years.

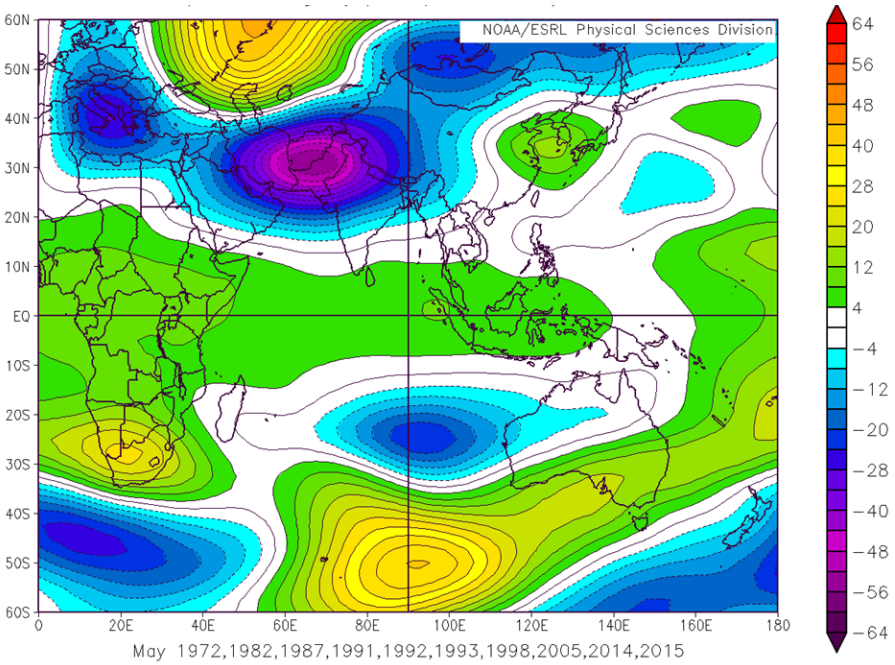


Figure 18. 200 mb geopotential height anomalies (Z200, m) in May during late onset years.

## 6. SST

The SST anomalies (SSTAs) for the early and late years are strikingly opposite and very similar to the SSTAs associated with La Niña and El Niño, respectively (Figures 19–20). The SSTAs were positive (negative) near the MC for the early (late) years, consistent with the idea that early (late) years are associated with anomalously strong (weak) convection near the MC. The SSTAs in the NWIO near HOA were negative (positive) for the early (late) years, consistent with the stronger (weaker) winds during those years. Note also that the strongest SSTAs for both the early and late composites occurred in the central-eastern tropical Pacific and the central North Pacific.

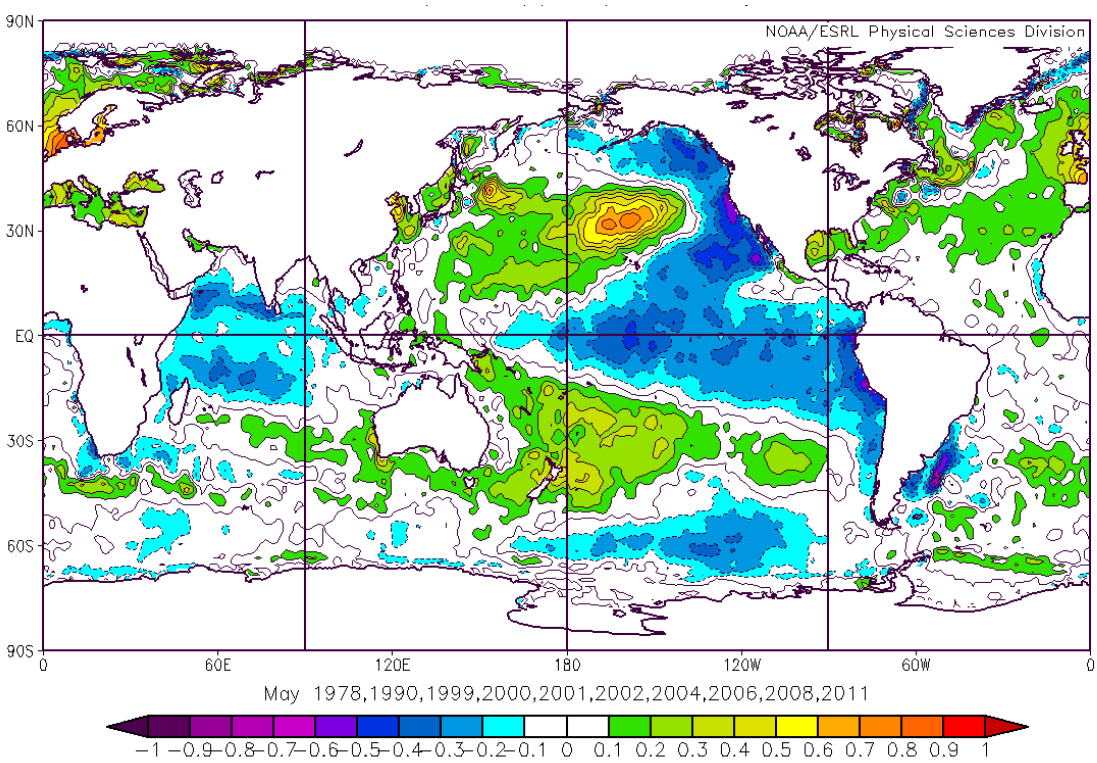


Figure 19. SST anomalies (℃) in May during early onset years.

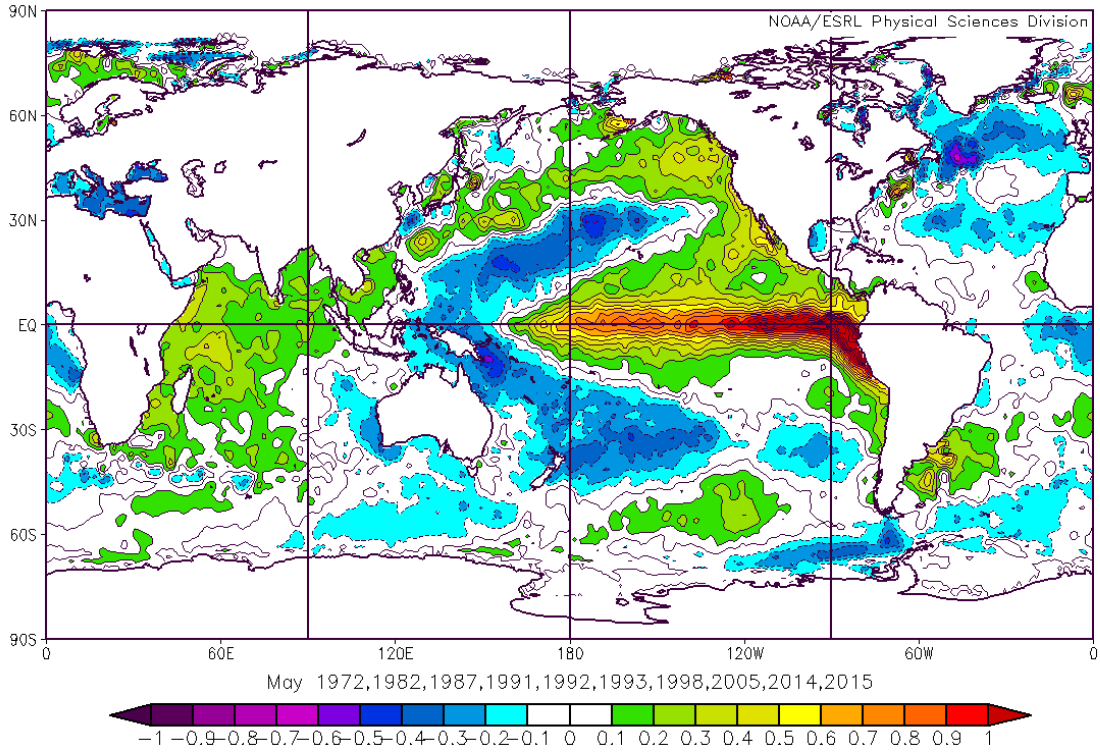


Figure 20. SST anomalies (℃) in May during late onset years.

Table 2 summarizes the conditional composite anomaly results shown in Figures 19–20, and highlights the tendency for the early and late anomalies to be opposite over a large portion of the global tropical-subtropical atmosphere and ocean. This indicates that early and late onsets tend to be part of global scales processes that end up influencing the onset. These processes likely include ENLN, MJO, IOD, and other processes that affect the tropics, especially SSTs and tropospheric convection in the Indo-Pacific region.

Table 2. Comparison of anomalies during early and late onset years.

| Variable | Early onset anomalies | Late onset anomalies |
|---|---|---|
| SLP over southern Asia | Negative | Positive |
| 1000 mb winds off HOA | Northeastward | Southwestward |
| SWH off HOA | Positive | Negative |
| Z850 over south Asia | Negative | Positive |
| Z200 over south Asia | Positive | Negative |
| SST tropical central-eastern Pacific | Negative | Positive |

## C. CORRELATIONS

We conducted a number of correlation experiments (see Table 1) to identify the relationships between the SWM onset off HOA and other variables, and to investigate dynamical processes that might explain those relationships. We focused on correlations between the predictand V and global SST because: (a) our conditional composite results showed a clear and dynamically plausible connections between those variables; and (b) many prior studies have shown that SST can be a good predictor of interannual climate variations at S2S lead times (e.g., Heidt 2009; Lemke 2010). Figure 21 shows the correlation between the predictand V and global SST, with SST leading by 0, 2, 4, and 6 months based on predictand V data from May of 1970–2017 and SST data from November-May of 1969–2017. Areas of positive (negative) correlation indicate that the SST in that region tended to vary in phase (out of phase) with the predictand V. For example: (a) the area of negative correlation in the central-eastern tropical Pacific indicates that when the SST there is low (high), the V predictand off HOA in May tends to be strong (weak), which corresponds to an early (late) SWM onset off HOA; and (b) the area of positive correlation in the central North Pacific indicates that when the SST there is low (high), the V predictand off HOA in May tends to be weak (strong), which corresponds to a late (early) SWM onset off HOA. Note that the correlation patterns are similar to the SSTA patterns shown in Figures 19–20. Also note the areas of persistent large magnitude correlations at all leads located in the central-eastern tropical Pacific and the central North Pacific. The correlations magnitudes near HOA are high at shorter lead

times but low at longer lead times. Together, these results indicate that SST variations, especially remote SSTs related to ENLN, are important in setting up processes during the northern fall and winter that then affect the onset of the SWM off HOA in the following northern spring. In addition, these results suggest that other climate variations that affect SSTs (especially SSTs near the MC and in the tropical Pacific) may be important in determining the SWM onset off HOA (e.g., MJO, IOD).

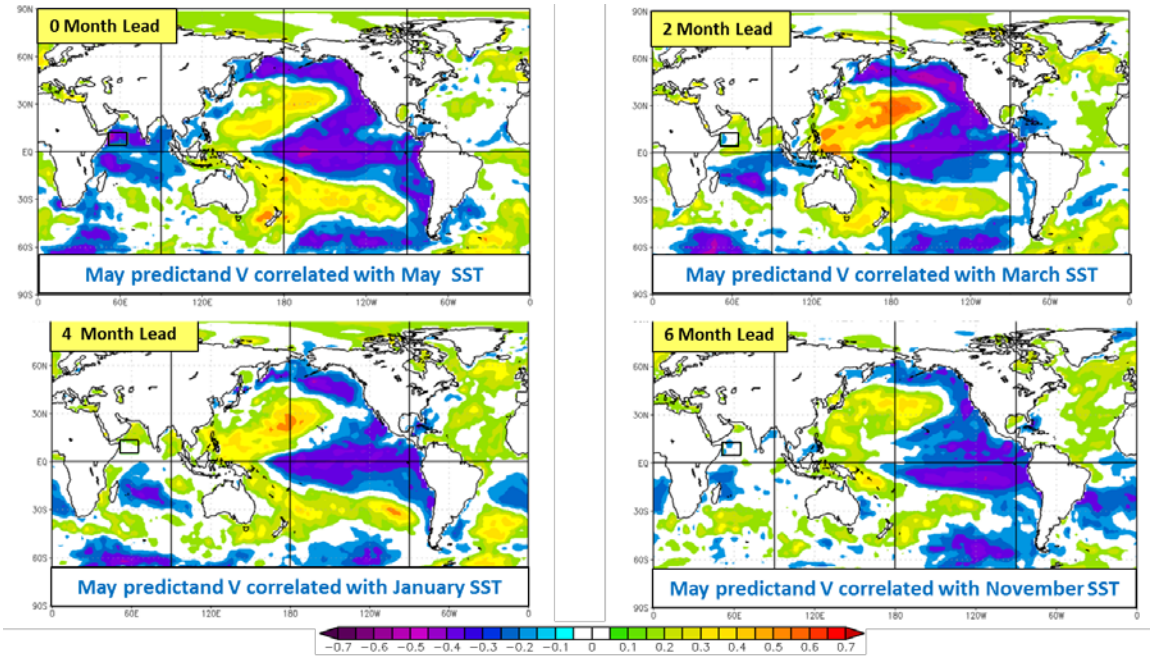


Figure 21. Correlations of the May predictand V winds off HOA (black box) to global SST, with SST leading by 0, 2, 4, and 6 months.

## D. PREDICTOR SELECTION

We used the correlation results, such as those in Figure 21, to identify potential predictors to test via tercile matching hindcasts (see Chapter II, section D.5). Figure 20 shows the two predictors on which we focused: (1) SST area averaged for the region 28°N-38°N, 178°E-165°W (the blue box in Figure 22); and (2) SST area averaged for the region 8°N-8°S, 162°W-148°W (the gold box in Figure 22). The correlations between SST in these two regions and the V predictand tended to be strong and significant at all lead times (see Figure 21). These predictors did not have the highest magnitude

correlations at all lead times, but they tended to have the overall highest magnitude correlations when considering all of the lead times, 0 to 6 months.

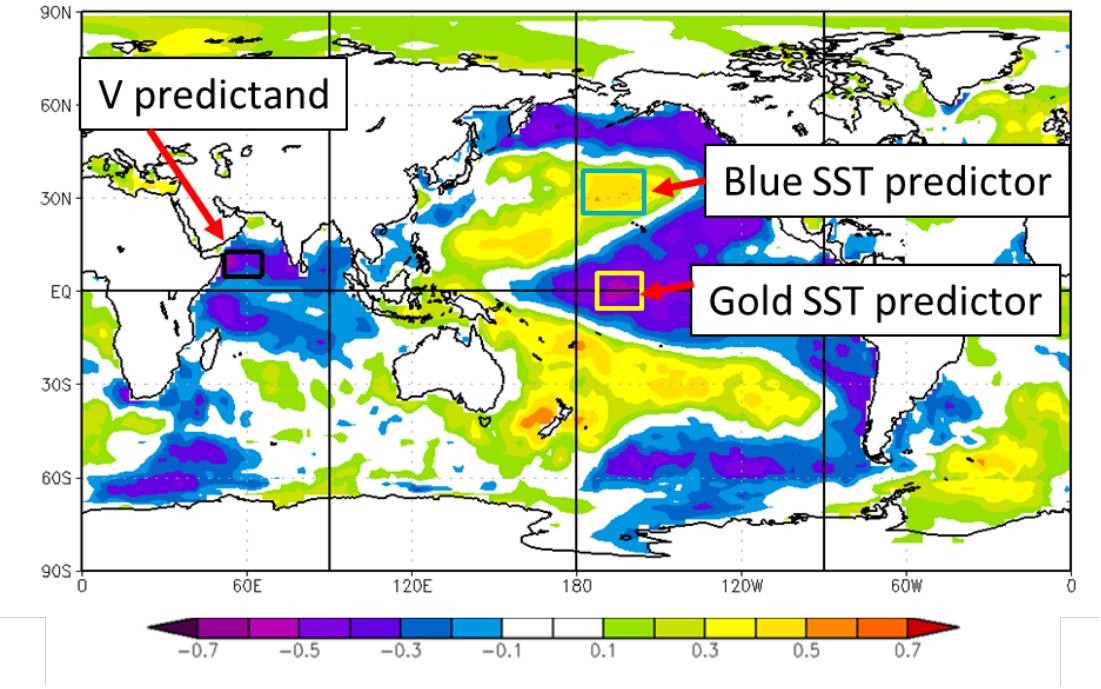


Figure 22. Correlation of May predictand V winds off HOA (black box) with global May SST (same as upper left panel in Figure 21). The blue and gold boxes represent two SST predictor regions.

## E. HINDCASTS

We applied the gold and blue SST predictors in tercile matching hindcast experiments (see Chapter II, section D.5). Each predictor was used to hindcast the V predictand for May of 1970–2017, for a total of 48 hindcasts for each predictor. The percent hit rates by lead time for each predictor, for all years, and for the AN years, the NN years, and the BN years, are shown in Table 3. The highest hit rate at each lead time is underlined. The percent hit rate varies by predictor, by lead time, and by grouping of years --- ranging from a low of about 19% to a high of about 81%. The hit rates were, in general, highest for: (a) short leads; and (b) BN events. The lowest hit rates were for NN events. At shorter (longer) leads, the gold (blue) SST predictor tended to have higher hit

rates than the blue (gold) SST predictor. These results indicate that SST predictors have the potential to be useful in S2S forecasting of the SWM onset off HOA. However, more work is needed, especially to investigate, for example: (a) alternative oceanic and/or atmospheric predictors; (b) applications of alternative hindcasting methods (e.g., regression, time-lagged ensemble hindcasting, optimal climate normals, and other statistical and dynamical methods (e.g., Wilks 2006)); (c) the use of multiple predictors (e.g., multi-variate predictors); (d) varying the choice of predictor by lead time; and (e) alternative verification metrics.

Table 3. Percent hit rates for the blue predictor box (blue cells) and gold predictor (gold cells) by lead time and divided into the 48 year average rates, and the rates for early, normal, and late onsets (i.e., the hit rates for the AN, NN and BN tercile categories). The bold underlined values indicate the highest percent hit rate for the given lead time and predictor.

| Lead Time | 48 Year Average | Early Onset | Normal Onset | Late Onset | 48 Year Average | Early Onset | Normal Onset | Late Onset |
|---|---|---|---|---|---|---|---|---|
| 0 | 62.5 | 62.5 | 56.3 | **68.8** | 64.6 | 50 | 62.5 | **81.3** |
| 1 | 50 | 56.3 | 31.3 | **62.5** | 58.3 | 56.3 | 50 | **68.8** |
| 2 | 37.5 | 43.8 | 18.8 | **50** | 52.1 | 56.3 | 37.5 | **62.5** |
| 3 | 33.3 | 37.5 | 18.8 | **43.8** | 56.3 | 56.3 | 50 | **63.5** |
| 4 | 50 | **56.3** | 50 | 43.8 | 47.9 | **56.3** | 37.5 | 50 |
| 5 | 43.8 | **50** | 31.3 | **50** | 47.9 | **50** | 43.8 | **50** |
| 6 | 56.3 | **56.3** | **56.3** | **56.3** | 45.8 | 43.8 | 43.8 | **50** |

We also investigated the relationships between ENLN events and early/late SWM onsets off HOA by identifying the years shown in Figure 7 that were EN, neutral, and LN years. A summary of these comparisons is shown in Figure 23, where the years in which EN, neutral, or LN conditions existed in May are marked. The intensity of the EN and LN conditions in May is marked as strong (S), moderate (M), or weak (W). Note that the AN (BN) tercile and early (late) onsets have a general association with LN (EN) conditions, and that the NN years tend to be associated with neutral conditions. These results support the idea that ENLN is important in determining early, normal, and late

onsets of SWM onset off HOA in May, but that other factors also determine the onset. This assessment of the importance of ENLN would be improved by extending it to show the ENLN conditions in the months preceding May (e.g., November-April). The conditions in these prior months are likely to be important in determining the onset in May, as indicated by the results shown in Table 3.

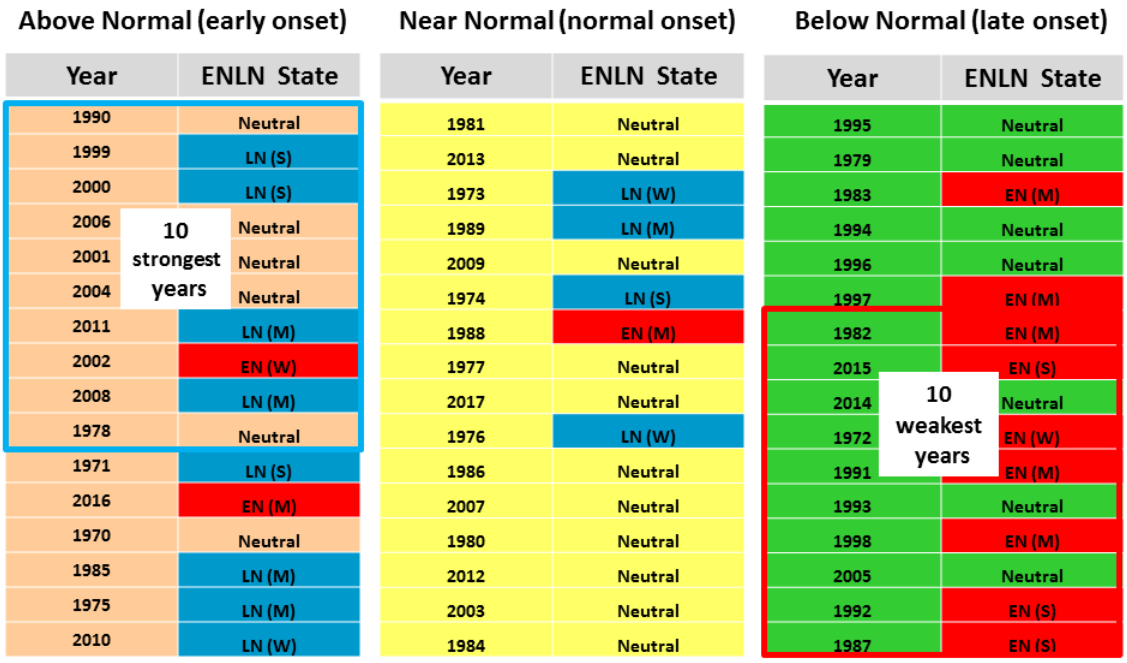


Figure 23. Predictand V values for 1970–2017 binned into above normal, near normal, and below normal terciles (left/peach column, middle/yellow column, and right/green column, respectively), corresponding to early, normal, and late onset years. The ten years with the highest (lowest) V predictand values are marked by a blue (red) box. Years in which EN, neutral, or LN conditions existed in May are marked as EN, neutral, or LN, respectively. The intensity of those EN and LN conditions is also indicated (S: strong, M: moderate, W: weak).

# IV. SUMMARY, CONCLUSIONS AND RECOMMENDATIONS

## A. SUMMARY

We investigated the potential for S2S forecasting of the onset of SWM surface winds and ocean surface waves off HOA by analyzing global atmospheric and oceanic variables, and three onset states: early, normal, and late. We examined statistical and dynamic relationships between the SWM winds in May off HOA and atmospheric and oceanic variables elsewhere in the world. We found that anomalous convection over south Asia, anomalous convection near the MC, and anomalous SSTs in the tropical and subtropical Pacific, were associated with onset anomalies. We found an association between La Niña (El Niño) events and early (late) onsets. Anomalies in the Mascarene High were not clearly linked to onset anomalies. Tropical Rossby-Kelvin wave dynamics may explain much of the mechanism that allows remote conditions to affect the onset off HOA at S2S lead times. S2S hindcasts of the onset based on SST in the central-eastern tropical Pacific and subtropical North Pacific indicate that the onset is predictable at S2S lead times. However, additional work is needed to develop methods for high skill S2S forecasting of the onset.

## B. CONCLUSIONS AND RECOMMENDATIONS

We developed initial answers to our research questions (Chapter I, section C). In particular, we determined that the onset of the SWM low level winds and ocean surface waves off HOA have the potential to be skilfully predicted at S2S lead times. We also determined that statistically significant and dynamically interpretable relationships (teleconnections) exist between the onset region and south Asia, the MC, and the tropical and subtropical Pacific at S2S lead times. These relationships support the assumption that skillful S2S predictions of the onset off HOA are possible. More research is needed to clarify and extend these relationships, and to exploit them for use in developing a S2S forecasting process. For example, the role of other climate variations, such as the MJO and IOD, should be investigated. The role of multiple simultaneous climate variations should also be addressed (Ilczuk 2016). The impacts of the northeast monsoon over Asia

in the preceding winter in creating precursor conditions that favor early or late onsets should be investigated. Additional predictors and combinations of predictors shpould be considered, as well as alternative forecasting methods (e.g., regression, lagged ensembling, optimizing and varying the predictor by lead time). We focused on the onset winds off HOA, but the corresponding ocean surface waves should be addressed in more depth. We also recommend using data sets with higher temporal resolution (weekly to daily resolution) to better determine the timing of the onset and associated dynamical processes. Finally, we suggest that research be done to determine if and how early and late onsets off HOA in May are related to the: (a) intensity of the SWM off HOA in June-September; and (b) the demise of the SWM off HOA in September-October.

# LIST OF REFERENCES


Beattie, J. C., 2015: Western North Pacific monsoon depressions: Formation, structure and transition to tropical cyclones. M.S. Thesis, Department of Meteorology, Naval Postgraduate School, 80 pp.

Budzko, D. C., 2005: North Pacific tropical cyclones and teleconnections. M.S. Thesis, Department of Meteorology, Naval Postgraduate School, 90 pp.

BOM, 2017: About the Maritime Continent. Accessed 05 December 2017. http://www.bom.gov.au/climate/about/tropics/maritime-continent.shtml

CEFA 2017: Climate, Ecosystem and Fire Applications. Retrieved from CFS Weekly to Seasonal Forecasts: https://cefa.dri.edu/CFS/cfs.php

CENTCOM 2017: U.S. Central Command. Accessed 05 December 2017, www.centcom.mil.

Chakraborty, A., and S. Agrawal, 2017: Role of west asian surface pressure in summer monsoon onset over central India. Environmental Research Letters, 12. Bengaluru, India: IOP Publishing.

ESRL/PSD, 2017: Multivariate ENSO Index (MEI). Accessed 02 March 2017, https://www.esrl.noaa.gov/psd/enso/mei/.

FNMOC, 2014: Fleet Numerical Meteorology and Oceanography Center Climatology Portal. Accessed 10 October 2017, https://portal.fnmoc.navy.mil/climoportal/index.htm.

Gill, A. E., 1982: Atmosphere-Ocean Dynamics. Academic Press. 662 pp.

Gillard, D. W., 1986: Contribution of atmospheric forcing to cooling of the Arabian Sea during onset of the southwest monsoon. M.S. Thesis, Department of Meteorology, Naval Postgraduate School, 75 pp.

Goswami, B. N., 2005: South Asian Summer Monsoon: An Overview. WMO Report of the International Committee of the Third International Workshop on Monsoons (IWM-III) .

Hastenrath, S., 1985: Climate and circulation of the Tropics. Dordrecht/Boston/Lancaster/Tokyo: D. Reidel Publishing company.

Heidt, S. L., 2009: Long-range atmospheric-ocean forecasting in support of undersea warfare operations in the western north Pacific. M.S. Thesis, Department of Meteorology, Naval Postgraduate School, 60 pp.

Ilczuk, R. E., 2016: The impacts of multiple simultaneous climate variations. M.S. Thesis, Department of Meteorology, Naval Postgraduate School, 90 pp.

Kalnay, E., and Coauthors, 1996. The NCEP/NCAR 40-Year Reanalysis Project. Bull. Amer. Meteor. Soc, 437–471.

Karmakar, S., 2015: Forecasting of southwest monsoon over south Asia and its socio-economic aspects. ResearchGate, 27–40.

Kistler, R., and Coauthors, 2001: The NCEP–NCAR 50-Year Reanalysis: Monthly Means CD-ROM and Documentation. Bull. Amer. Meteor. Soc., 82, 247–267.

Krishnamurti, T. N., P. Ardanuy, Y. Ramanathan, and R. Pasch, 1981: On the onset vortex of the summer monsoon. Mon. Wea. Rev., 109, 344.

Lau, K. M., N. C. Lau, and S. Yang, 2005: Current Topics on Interannual Variability of the Asian Monsoon. The Global Monsoon System: Research and Forecast, 440–454.

Lau, N. C., and B. Wang, 2005: Monsoon-ENSO Interactions. The Global Monsoon System: Research and Forecast, 299–309.

Lau, N. C., and M. J. Nath, 2000: Impact of ENSO on the variability of the Asian-Australian monsoons simulated. J. Climate.

Lemke, B. D., 2010: Long-range forecasting in support of operations in the Horn of Africa. M.S. Thesis, Department of Meteorology, Naval Postgraduate School, 80 pp.

Met Office Hadley Centre., 2016: Met Office Hadley Centre observations datasets. Accessed 10 February 2016, https://www.metoffice.gov.uk/hadobs/hadisst/.

Murphree, T., 2017a: MR3610 course module 7: Seasonal Cycles, Part 1. Department of Meteorology, Naval Postgraduate School, Monterey, California.

Murphree, T., 2017b: MR3610 course module 13: Rossby Waves and Climate. Department of Meteorology, Naval Postgraduate School, Monterey, California.

Murphree, T., 2017c: MR3610 course module 15. Teleconnections. Department of Meteorology, Naval Postgraduate School, Monterey, California.

Murphree, T., 2017d: MR3610 course module 16: El Nino La Nina Southern Oscillation, Part 1. Department of Meteorology, Naval Postgraduate School, Monterey, California.

NGA 2010: Maritime safety information. Accessed 02 February 2017, www.msi.nga.mil.

NOAA/ESRL PSD, 2017: Linear Correlations in Atmospheric Seasonal/Monthly accessed 14 October 2017, https://www.esrl.noaa.gov/psd/data/correlation/.

NOAA/NCEI, 2017: Climate Prediction Center. Accessed 02 December 2017, https://www.ncdc.noaa.gov/teleconnections/enso/indicators/sst.php.

NOAA/EMC, 2017a: WAVEWATCH III® Model accessed 30 March 2017, http://polar.ncep.noaa.gov/waves/wavewatch/.

NOAA/EMS. 2017b: WAVEWATCH III® Model accessed 30 March 2017, http://polar.ncep.noaa.gov/waves/wavewatch/.

Noska, R., and V. Misra, 2016: Characterizing the onset and demise of the Indian summer monsoon. Geophys. Res. Letters, 43, 4547–4554. doi:10.1002/ 2016GL068409.

Oo, S. M., 2007: Forecasting Southwest Monsoon Onset, Withdrawal Date and Rainfall for Myanmar. University of the Philippines, 1 p.

Parrish, K. A., 2015: Interannual variations in Arctic winter temperature: The role of global scale teleconnections. M.S. Thesis, Department of Meteorology, Naval Postgraduate School, 100 pp.

Raju, P., U. Mohanty, and R. Bhatla, 2004: Onset Characteristics of the Southwest monsoon over India. International J. Climate, 25, 167–182.

Robinson, P. J., and A. Henderson-Sellers, 1999: Contemporary Climatology (2nd ed.). Essex, England: Pearson prentice hall, 317 pp.

Saha, S., and Coauthors, 2010: NCEP Climate Forecast System Reanalysis (CFSR) Selected Hourly Time-Series Products, January 1979 to December 2010. NCAR Computational and Information Systems Laboratory Research Data Archive, accessed 11 February 2016, https://doi.org/10.5065/D6513W89.

Saha, S., Shrinivas, M., Wu, X., Wang, J., Nadiga, S., Tripp, P., . . . Becker, E., 2014. The NCEP Climate Forecast System Version 2. *J. Climate*, **27**, 2185–2208.

Schneller, R. J., 2007: Anchor of Resolve: A History of U.S. Naval Forces Central Command fifth Fleet. Military Bookshop, 144 pp.

Stone, M. M., 2010: Long-range forecasting of Arctic sea ice. M.S. Thesis, Department of Meteorology, Naval Postgraduate School, 60 pp.

University of Texas at Austin: Large Map of IO, accessed 01 December 2017, www.lib.utexas.edu/maps/indian_ocean.html.

U.S. NAVCENT, 2017: Combined Maritime Forces (CMF). Accessed 12 March 2017, http://www.cusnc.navy.mil/Combined-Maritime-Forces/.

Walker, G. T., 1924: Correlation in Seasonal Variations of Weather, IV, A Further Study of World Weather. Indian Meteorology Dept.

Webster, P. J., V. Magana, T. Palmer, J. Shukla, R. Tomas, M. Yanai, et al., 1998: Monsoons: Processes, predictability and the prospects for prediction. J. Geophys. Res, 103, 14,451-14,510.

Wikimedia Commons, 2017a. Category: Images. Accessed 02 December 2017. www.commons.wikimedia.org/wiki/File:horn_of_africa_states.svg.

Wikimedia Commons, 2017b. Category: Images. Accessed 02 December 2017. www.commons.wikimedia.org/wiki/File:nasa_horn_of_africa.jpg.

Wikimedia Commons, 2017c. Category: Images. Accessed 02 December 2017. www.upload.wikimedia.org/wikipedia/commons/6/6b/indo-Pacific_biogeographic_region_map-en.png.

Wilks, D., 2006: Statistical Methods in the Atmospheric Science (2nd ed.). Academic Press, 627 pp.

Wolter, K., and M. Timlin, 2011: El Nino/Southern Oscillation behavior since 1871 as diagnosed in an extended Multivariate ENSO Index (MEI). International J. Climate, 31, 1074–1087.

# INITIAL DISTRIBUTION LIST

1. Defense Technical Information Center
   Ft. Belvoir, Virginia

2. Dudley Knox Library
   Naval Postgraduate School
   Monterey, California